

Supporting Information

Ables et al. 10.1073/pnas.1717506114

SI Materials and Methods

Animals. Animal experiments were performed in strict accordance with the National Institute of Health Guide for the Care and Use of Laboratory Animals and were approved by the Institutional Animal Care and Use Committee at The Rockefeller University. Animals were housed in a specific pathogen-free facility, with ad libitum access to food and water, and maintained on a 12-h light/dark cycle, with lights on at 7 AM. Male and female transgenic mice were bred in our facility. Animals were group housed (unless otherwise specified) and were 8 wk or older at the beginning of each experiment. Male mice between 10 and 20 wk were used for behavioral assays. Male and female mice at least 8 wk old were used for TRAP studies. BAC transgenic mice were generated by GENSAT (GENSAT.org) and the following mouse lines were used in this study: *Amigo1*-Cre (NP231), *Amigo1*-eGFP (FL213), *Epyc*-Cre (KR363), *Chrna5*-Cre (SN83), *Chrna5*-eGFP (IG16), *Epyc*-eGFP (DA4), *Chat*-TRAP (DW167), *Slc6a3*-TRAP (JD1640), *Slc6a4*-TRAP (JD60), and *Drd1*-TRAP (CP73). Cre mouse lines were backcrossed at least six generations to C57BL/6J (Jackson stock no. 000664) before behavioral studies. eGFP mouse lines were maintained on a mixed background. In addition, *Chat*-ChR2-eYFP mice (Jackson stock no. 014546) were purchased from The Jackson Laboratory. Finally, a Cre-dependent mouse line carrying a flox-STOP-flox allele of eGFP-tagged ribosomal protein L10a in the *Eef1a1* locus was obtained from the Jeffrey Friedman laboratory. Mice were genotyped by PCR on genomic tail DNA for Cre or GFP using primers from the Washington University Genotyping Core Facility (mgc.wustl.edu/protocols/pcr_genotyping_primer_pairs).

Stereotaxic Viral Injection. Adult mice weighing 25 g or more (7–8 wk of age, or older) were anesthetized using a mixture of ketamine/xylazine (12 mg/mL ketamine, 10 mg/mL xylazine in sterile 0.9% saline, i.p.) and positioned in a stereotaxic frame (Kopf Instruments or Stoelting Instruments) with the incisor bar set to the “flat-skull” position (i.e., difference between Bregma and lambda <0.1). A single incision was made in the scalp and a small burr hole was drilled into the skull at the site of injection. Viruses were administered using a pulled glass capillary with a hydrolic-driven plunger (Narishiga, MO10) at a rate of 0.1 μ L/min. The glass capillary was left in place for a minimum of 5 min after injection. Viral injections into the interpeduncular nucleus were made at the following coordinates: anterior/posterior (AP) –3.6 mm from Bregma, medial/lateral (ML) –1.7 mm from midline, dorsal/ventral (DV) –4.98 from brain surface, with the needle angled 20° to avoid the sagittal sinus. Incisions were closed using VetBond (3M). Animals were allowed to recover for at least 1 wk before behavioral testing. A minimum of 2 wk was allowed for AAV viral expression. Viral placement was confirmed via IHC and mice without appropriate expression were excluded. A minimum of 4 wk was allowed between AAV and rabies injections.

Viruses. The following viral vectors were purchased from the University of Pennsylvania Viral Vector Core: adeno-associated virus (AAV) 2/8 DIO-PE, -APC, and -mCherry; AAV2/9 DIO ChR2-mCherry, eGFPL10a; AAV2/5 DIO ChR2-mCherry, PE, MPE. The following viral vectors were purchased from the University of North Carolina Viral Vector Core: AAV 2/8 DIO-RG, -TVA-mCherry. Envelope A G-deleted rabies-eGFP was purchased from the Salk Institute. Viral titers were in the range of 10^{12} to 10^{13} inclusion forming units (IFU)/mL AAV 2/8 NOS1-siRNA was purchased from Vector Biolabs. Animals infected with AAV were maintained in an animal biosafety level 2

(ABLS2) facility for 72 h before returning to normal housing conditions. Following infection with rabies virus, animals were housed in an ABL2 until killing 7 d later.

Immunohistochemistry. The primary antibodies used were: rabbit polyclonal anti-RFP (1:1,000, ab62341; Abcam), goat polyclonal anti-CHAT (1:500, AB144P; Millipore), chicken polyclonal anti-GFP (1:1,000; Aves Labs), goat polyclonal anti-NOS1 (1:300, ab1376; Abcam), rat monoclonal anti-SST (1:100, MAB354; Millipore), and rabbit monoclonal anti-SSTR2 (1:100, ab134152; Abcam). Free-floating sections were blocked in PBS or TBS with 3% normal donkey serum and 0.3% Triton X-100 for 1 h at room temperature, before incubation with primary antibodies diluted with blocking solution overnight at room temperature. Following primary incubation, sections were rinsed with PBS and then incubated with secondary antibodies (1:500; Jackson Immuno-Research) for 1–4 h at room temperature, washed, and then mounted on slides and coverslipped in DAKO fluorescent mounting media. For SST staining, free-floating sections were incubated in TBS blocking solution (cat. no. 37535; Thermo Fisher Scientific) for 1 h and then incubated with primary antibody diluted in TBS blocking solution for three nights at 4 °C. Heat-mediated antigen retrieval, 15 min at 95 °C in citric acid (pH 6.0), was performed on slide-mounted sections before incubation with the CHAT and SSTR2 antibodies overnight at room temperature. Fluorescent signals were detected using a confocal laser scanning microscope (Zeiss LSM700). For quantification of fluorescence intensity, all sections in the experiment were stained at the same time and imaged using the same settings. Initial settings were established using a control animal. Fluorescence intensity was quantified on a whole image field of four to six IPN sections per animal using Zeiss ZEN2 software and calculated as the average intensity per section.

Drugs. (–)-Nicotine hydrogen tartrate salt was purchased from Sigma-Aldrich. (–)-Nicotine hydrogen tartrate salt was dissolved in 0.9% sterile saline for 0.3-mg/mL stock solution, pH adjusted to ~7.4 and injected at 10 mL/kg volume (0.35 mg/kg free base). For chronic nicotine administration via drinking water, (–)-nicotine hydrogen tartrate salt was dissolved in 0.2% saccharin in tap water for 500-mg/L solution. Solutions were changed at least weekly. Mice were single-housed and bottles weighed daily to measure consumption.

TRAP and RNA-Seq. The IPN of four to six animals were grossly dissected and pooled per biological replicate. TRAP was performed as previously described (1) with the following modifications: Homogenization volume was reduced to 1 mL and the volume of beads used was reduced to 150 μ L. RNA was isolated using Qiagen RNeasy Micro kit and cDNA was prepared using Ovation RNA-Seq System V2 (cat. no. 7102; NuGEN) with the maximum recommended input volume. RNA-Seq reads were aligned to the University of California Santa Cruz (UCSC) mm10 reference genome using STAR (2), version 2.3.0e_r291, with default settings. Quantification of aligned reads was done using htseq-count module, part of the HTSeq framework (3), version 0.6.0, using default settings, with “union” mode to handle reads overlapping more than one feature. Differentially expressed genes were identified by performing a negative binomial test using DESeq2 (4) (R-package version 1.4.5) with default settings. Significant *P* values were corrected to control the false discovery rate of multiple testing according to the Benjamini–Hochberg

procedure at 0.05 threshold and minimum threshold of 0.6 log₂ fold change.

Slice Preparation and Electrophysiological Recordings. Adult mice were killed by cervical dislocation and brains were dissected in chilled solution (4 °C) containing (in millimoles): 87 NaCl, 2 KCl, 0.5 CaCl₂, 7 MgCl₂, 26 NaHCO₃, 1.25 NaH₂PO₄, 25 glucose, 75 sucrose, bubbled with a mixture of 95% O₂/5% CO₂. The 250- μ m coronal IPN-containing slices were cut with a VT1000S vibratome (Leica), preincubated for 30 min at 37 °C, and then transferred to the recording solution containing (in millimoles): 125 NaCl, 2.5 KCl, 2 CaCl₂, 1.3 MgCl₂, 26 NaHCO₃, 1.25 NaH₂PO₄, 10 glucose, 2 sodium pyruvate, 3 myo-inositol, 0.44 ascorbic acid, bubbled with a mixture of 95% O₂/5% CO₂. Slices rested in this recording solution at room temperature for at least 1 h before recordings began.

For IPN characterizations, patch pipettes had resistances of 4–8 M Ω when filled with a solution containing (in millimoles): 105 K-gluconate, 30 KCl, 10 Hepes, 10 phosphocreatine, 2 ATP-Mg²⁺, 0.3 GTP (pH adjusted to 7.2 with KOH). For whole-cell recordings of the NO and SST effects, patch pipettes were filled with internal solution that contained the following (in millimoles): 130 K-gluconate, 10 Hepes, 0.6 EGTA, 5 KCl, 3 Na₂ATP, 0.3 Na₃GTP, 4 MgCl₂, and 10 Na₂-phosphocreatine. Cells were recorded at 30–36 °C. Electrophysiological responses were recorded with an EPC 10 patch-clamp amplifier and PatchMaster and FitMaster software (HEKA Elektronik).

To characterize IPN neuronal membrane properties, the following parameters were measured: V_{rest} (resting membrane potential), recorded immediately after whole-cell configuration was established; R_{in} (input resistance), determined from the voltage change upon –50 pA current pulse at resting membrane potential; τ_m (membrane time constant), determined at 63% of the maximal response to a –50-pA current pulse; and spike width: determined as spike width at the half maximum between action potential peak and threshold.

For puff applications, a second pipette was moved in close proximity of the patched cells. A total of 100 μ M nicotine was puff applied for 100 ms while neurons were clamped at –70 mV.

For indicated recordings, 0.3% biocytin was added to the intracellular recording solution. For morphological analyses of recorded neurons, slices were fixed for 20–30 min in 4% PFA following the recording. For biocytin staining, slices were washed with PBS and incubated with streptavidin-conjugated Alexa (1:500) and 0.3% Triton X-100 in PBS overnight. Slices were then washed with PBS and mounted on microscope slides. Confocal image stacks were acquired using a Zeiss LSM700 microscope.

Behavioral Procedures.

Nicotine CPP. Conditioned place preference was performed using a three-chamber apparatus from Med Associates, Inc. (MED-CPP-3013). Mice were allowed to habituate to the procedure room for at least 1 h before testing or conditioning. On the first day, mice were allowed to explore the entire apparatus for 20 min to obtain baseline preference to any of the three compartments. Groups were balanced such that there was no initial preference for nicotine-paired side. Conditioning trials occurred over 3 consecutive days, with two trials per day. Mice received saline i.p. during the morning conditioning session and were confined to one of the side compartment of the apparatus for 25 min. During the afternoon conditioning session, mice received nicotine i.p. and were confined to the opposite side compartment (drug-paired compartment) for 25 min. To minimize association of the compartments with pain of injection, the entire cage of mice was injected in their home cage and loaded into chambers after all mice were injected (~30 s after injection). On the test day (day 5), mice

were allowed to explore the entire apparatus for 20 min and time spent in each compartment was assessed. Nicotine preference was calculated as the time spent in the drug-paired chamber on the last day minus the time spent in the drug-paired chamber on the first day.

Open field and light/dark. Locomotor activity was measured in eight identical open field boxes (50 \times 50 \times 22.5 cm) equipped with two rows of infrared photocells placed 20 and 50 mm above the floor (Accuscan and Omnitech Electronics). Mice were placed in the center of the field and activity was recorded by Fusion Software for 30 min. Distance traveled and time spent in the center were calculated. For light/dark, an enclosed insert was placed in one half of each open field box with an opening in the center of the open field arena. Mice were placed into the dark enclosed side of the chamber and allowed to freely explore for 10 min. Distance traveled and time spent in the open (light) and enclosed (dark) sides was calculated.

Elevated plus maze. Elevated plus maze was used to assess anxiety-like behavior. The apparatus consisted of a central platform (5 \times 5 cm), two opposed open arms (25 \times 5 cm) and two opposed closed arms with 15-cm-high black walls. The edges of the open arms were raised 0.25 cm to decrease the chance of a mouse falling. Mice were placed on the central platform and the time and activity were recorded for 10 min via a camera positioned above the apparatus. Time spent in each arm and the distance traveled was recorded automatically using EthoVision XT tracking software (Noldus).

Prepulse inhibition. Startle reflexes were measured in four identical startle response SRLAB apparatus (San Diego Instruments). Each system contained a Plexiglas cylinder, 5.5 cm in diameter and 13 cm long, mounted on a platform located in a ventilated, sound-attenuated chamber. Startle responses were transduced by piezoelectric accelerometers mounted under each platform. Output signals were digitized and the average startle response and maximum amplitude of the startle response were recorded as startle units. The startle session began with a 5-min acclimation period in the presence of a 65-dB background white noise, followed by presentation of 5 120-dB pulse trials to ensure a stable baseline and reduce variability. Afterward, mice were presented with four startle stimuli of different intensities (80, 90, 100, 110, and 120 dB). A total of 20 trials in a pseudorandomized manner with an average intertrial interval of 15 s (range: 6–21 s) were presented. Amplitude of startle was measured within a 100-ms window following the stimuli. Prepulse inhibition (PPI) was examined using prepulses of 3, 6, or 12 dB (20 ms) above background. Testing consisted of 12 120-dB pulses (40-ms duration) alone and 10 pulses preceded (100 ms) by each prepulse (20-ms duration). One last block of 5 120-dB pulses was presented to ensure again a stable baseline. Percent PPI was calculated using the following formula: $100 \times (\text{startle alone} - \text{startle with prepulse/startle alone})$. PPI was reported as percent inhibition of the average startle response.

Forced swim. Mice were placed in a 2-L glass beaker filled with tap water set at room temperature (23–25 °C) for 6 min. Their escape-related mobility behavior was videorecorded and scored automatically using CleverSys software.

Statistical Analysis. Statistical analyses were performed with GraphPad Prism 7. Unpaired one-tailed (for CPP, as we expected the dose used to be rewarding) or two-tailed (for fluorescence intensity) Student *t* tests, two-way ANOVA or repeated measures (RM) two-way ANOVA were used for analyzing most of the data as indicated in figure legends, with the exception of TRAP data, which were analyzed after normalization using the DESeq2 method. Results are presented as means \pm SEM.

1. Heiman M, Kulicke R, Fenster RJ, Greengard P, Heintz N (2014) Cell type-specific mRNA purification by translating ribosome affinity purification (TRAP). *Nat Protoc* 9: 1282–1291.
2. Dobin A, et al. (2013) STAR: Ultrafast universal RNA-seq aligner. *Bioinformatics* 29:15–21.

3. Anders S, Pyl PT, Huber W (2015) HTSeq: A Python framework to work with high-throughput sequencing data. *Bioinformatics* 31:166–169.
4. Love MI, Huber W, Anders S (2014) Moderated estimation of fold change and dispersion for RNA-seq data with DESeq2. *Genome Biol* 15:550.

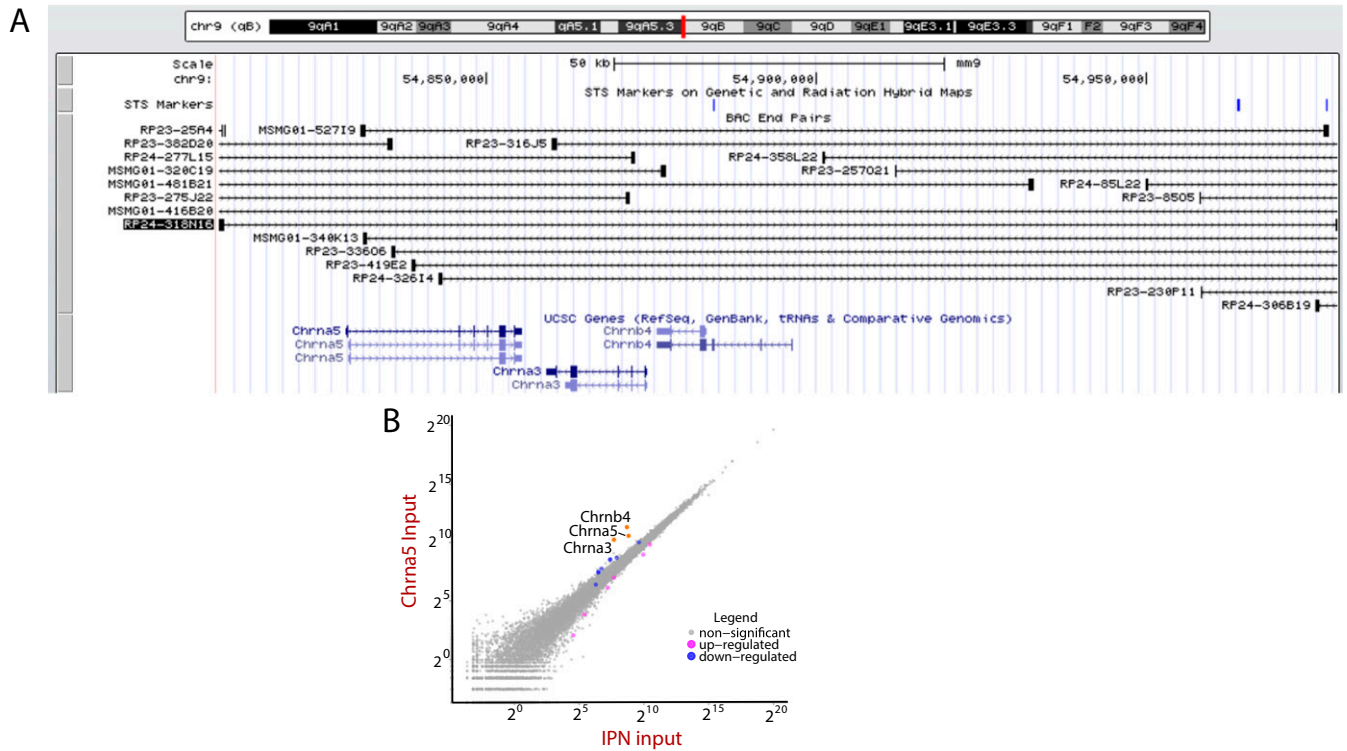


Fig. S1. Related to Fig. 1. *Chrna3-Chrna5-Chrnb4* gene cluster is overexpressed in *Chrna5-Cre* (SN83)::EH-EGFP-RPL10a mice. (A) UCSC genome browser map of BAC used to generate *Chrna5-Cre* mice shows that the *Chrna3-Chrna5-Chrnb4* gene cluster is included in the BAC. (B) Scatterplot of differential expression analysis of the inputs from pooled *Amigo1-Cre* (NP231)::EH-EGFP-RPL10a and *Epyc-Cre* (KR363)::EH-EGFP-RPL10a mice compared with *Chrna5-Cre* (SN83)::EH-EGFP-RPL10a mice. Note that levels of *Chrna3*, *Chrna5*, and *Chrnb4* are significantly higher in the *Chrna5* mice than the other lines.

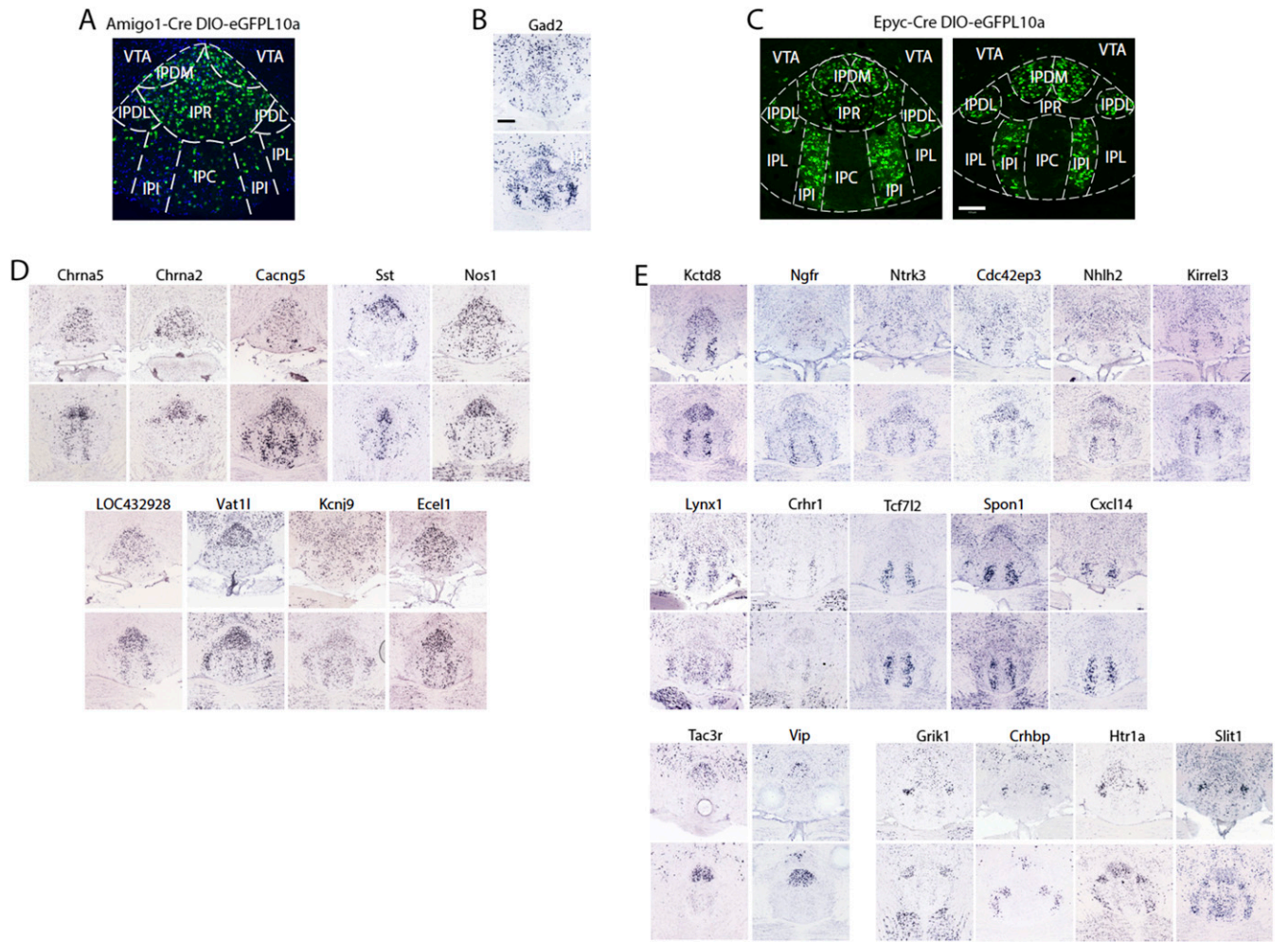


Fig. S2. Related to Fig. 1. Validation of TRAP by Allen Brain Atlas. (A) Confocal images of *Amigo1*-Cre::EH-EGFP-RPL10a IPN. (B) *Gad2* ISH at two different positions along rostral/caudal axis. (C) Confocal images of *Epyc*-Cre mice injected with AAV-DIO-EGFPL10a in the IPN. (Scale bar: 100 μ m.) (D) ISH images of several transcripts enriched in *Amigo1* cells with distribution in distinct subnuclei. (E) ISH images of several transcripts enriched in *Epyc* cells with distribution in distinct subnuclei. All ISH images are courtesy of Allen Brain Atlas.

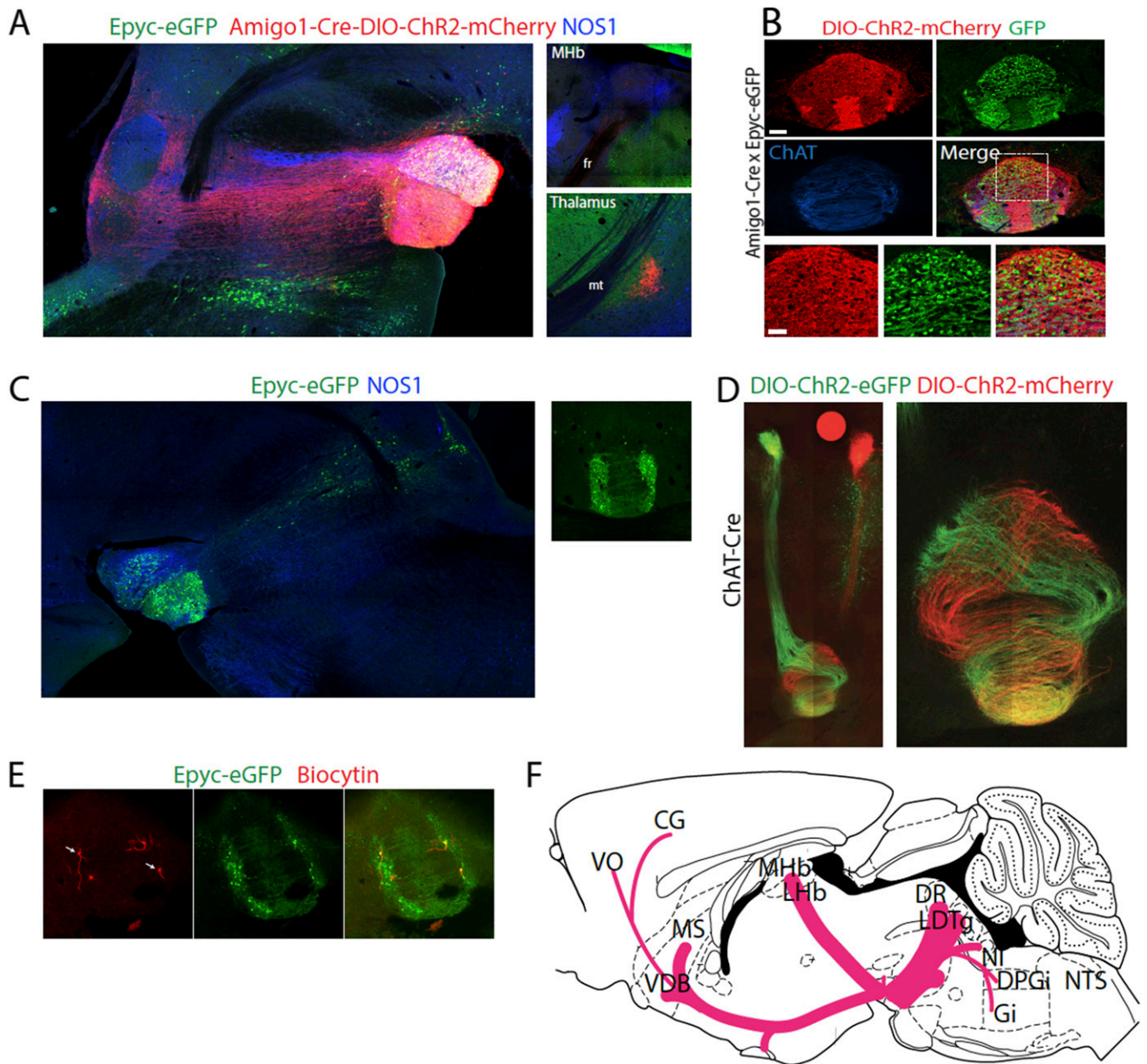


Fig. S3. Related to Fig. 2. $\alpha 5$ -*Amigo1* cells are the primary projection population, while $\alpha 5$ -*Epyc* cells are interneurons. (A) Sagittal section of *Amigo1*-Cre::*Epyc*-EGFP mouse injected with AAV-DIO-ChR2-mCherry and stained for NOS1. The $\alpha 5$ -*Amigo1* cells provide the majority of the projection to caudal structures. A minor ascending projection to the thalamus and MHB can also be seen (Right). (B) *Amigo1*-Cre mice were crossed to *Epyc*-EGFP mice to determine extent of overlap between the populations. Immunohistochemistry of coronal sections reveals very little colocalization of GFP and mCherry. Dotted line indicates area of higher magnification (Bottom). (Scale bar: low magnification 100 μ m, high magnification 50 μ m.) (C) Sagittal section of *Epyc*-EGFP mouse stained for NOS1. Note the sparse projection from IPN to caudal structures and projections between both IPI within IPN (Right). $\alpha 5$ -*Amigo1* cells appear to be a series of distinct populations along the IPN/DR axis. (D) Injection of *ChAT*-Cre mice with ChR2-EYFP in the Left MHB and ChR2-mCherry in the Right MHB demonstrates contribution of projections from each side to the IPN. (E) Streptavidin filling of *Epyc*-EGFP cells confirm that they are not projection neurons. (F) Schematic of inputs to IPN based on monosynaptic tracing. Note small input from PFC (VO), with larger inputs from the septum (MS, VDB), MHB, and caudal structures (DR, LDTg, NI, DPGi, Gi). Abbreviations are as follows: CG, cingulate gyrus; DPGi, dorsal paragigantocellular nucleus; DR, dorsal raphe; DTg, dorsal tegmentum; Gi, gigantocellular nucleus; IF, intrafascicular nucleus; LDTg, laterodorsal tegmentum; Lhb, lateral habenula; MHB, medial habenula; Mlf, medial longitudinal fasciculus; MS, medial septum; NI, nucleus incertus; NTS, nucleus tractus solitarius; PDTg, posteriodorsal tegmentum; PMnR, paramedian raphe; RLI, rostral linear nucleus; Th, thalamus; VDB, ventral diagonal band; and VO, ventral optic area.

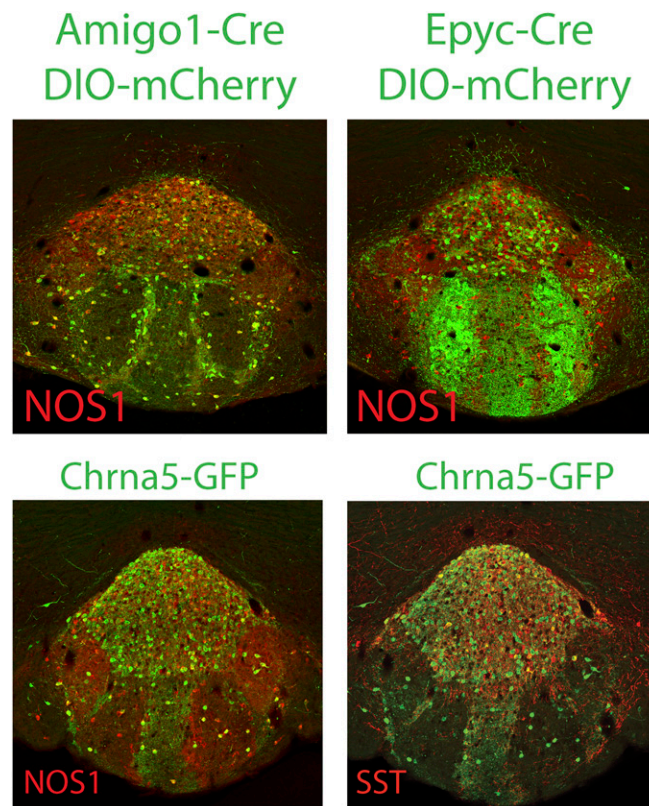


Fig. S4. Related to Fig. 3. Visualization of NOS1 and SST in $\alpha 5$ -*Amigo1* and $\alpha 5$ -*Epyc* cells. IHC of coronal sections confirms that NOS1 is expressed in $\alpha 5$ -*Amigo1* cells, but not in $\alpha 5$ -*Epyc* cells (Top). *Chrna5*-eGFP cells stain for both NOS1 and SST.

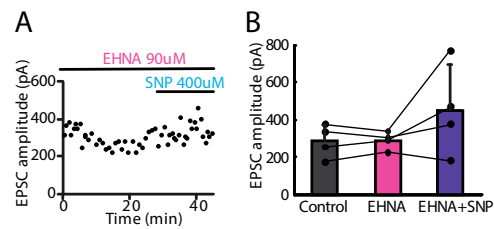
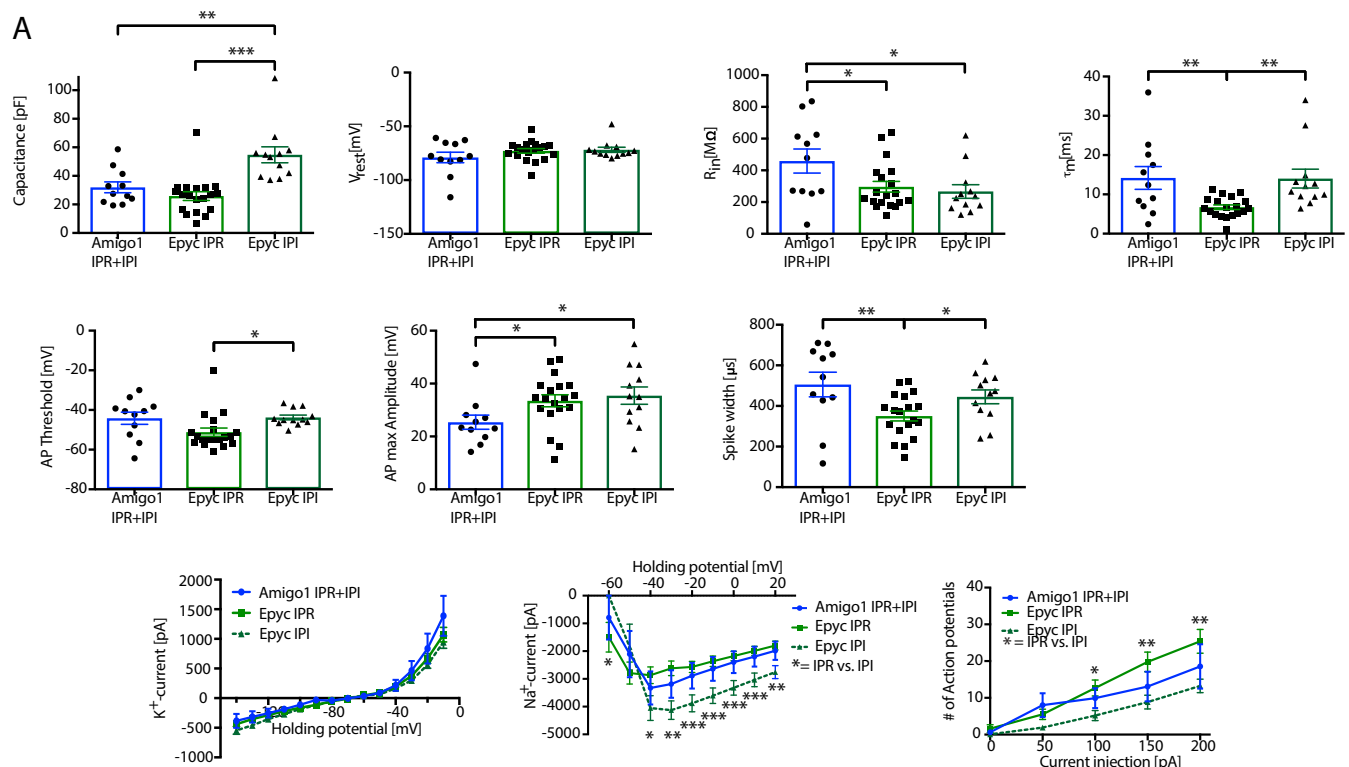


Fig. S5. Related to Fig. 4. (A) Application of the PDE2A inhibitor EHNA blocks reduction in glutamate release produced by the NO donor SNP. (B) Summary data show that EHNA blocks SNP-induced reduction in EPSCs.



B

Fig. S6. Related to Fig. 5. Electrophysiological characteristics of $\alpha 5$ -Amigo1 and $\alpha 5$ -Epyc cells. (A) Electrophysiological characteristics of $\alpha 5$ -Amigo1 and $\alpha 5$ -Epyc cells. (* $P < 0.05$, ** $P < 0.01$, *** $P < 0.001$, unpaired two-tailed t test). (B) Streptavidin-filled Epyc-eGFP neurons. See Fig. 4 for reconstruction of individual neurons.

- Dataset S1. Differential expression analysis of Chrna5 TRAP**
[Dataset S1](#)

- Dataset S2. Differential expression analysis of Chrna5-Cre (SN83) input vs. pooled Amigo1-Cre and Epyc-Cre IPN inputs**
[Dataset S2](#)

- Dataset S3. Differential expression analysis of Amigo1 TRAP**
[Dataset S3](#)

Dataset S4. Differential expression analysis of *Epyc* TRAP

[Dataset S4](#)

Dataset S5. Differential expression analysis of *ChAT* TRAP

[Dataset S5](#)

Dataset S6. Differential expression analysis of nicotine-treated *Amigo1* TRAP

[Dataset S6](#)

Dataset S7. Filtered differential expression analysis of nicotine-treated *Amigo1* TRAP exon (>100 base mean, $P > 0.05$)

[Dataset S7](#)

Dataset S8. Differential expression analysis of nicotine-treated *Amigo1* TRAP 3' UTR

[Dataset S8](#)

Dataset S9. Filtered differential expression analysis of nicotine-treated *Amigo1* TRAP 3' UTR (>100 base mean, $P > 0.05$)

[Dataset S9](#)

Dataset S10. Differential expression analysis of nicotine-treated *Epyc* TRAP

[Dataset S10](#)

Dataset S11. Filtered differential expression analysis of nicotine-treated *Epyc* TRAP (>100 base mean, $P > 0.05$)

[Dataset S11](#)

Dataset S12. Differential expression analysis of nicotine-treated *Epyc* TRAP (3' UTR)

[Dataset S12](#)

Dataset S13. Differential expression analysis of nicotine-treated *ChAT* TRAP

[Dataset S13](#)

Dataset S14. Filtered differential expression analysis of nicotine-treated *ChAT* TRAP (>100 base mean, $P > 0.05$)

[Dataset S14](#)

Dataset S15. Behavioral analysis of *Amigo1*-Cre and *Epyc*-Cre mice injected with tToxins

[Dataset S15](#)